Surface Structure and Coverage of an Oligonucleotide Probe Tethered onto a Gold Substrate and Its Hybridization Efficiency for a Polynucleotide Target

Eva Huang, Munlika Satjapipat, Shubo Han, and Feimeng Zhou*

Department of Chemistry and Biochemistry, California State University, Los Angeles, Los Angeles, California 90032

Received July 18, 2000. In Final Form: October 31, 2000

A single-stranded oligonucleotide whose 5′ end is derivatized with a mercaptohexyl tether group was either directly anchored onto a gold surface or attached to a gold surface as part of a mixed self-assembled monolayer that contains mercaptohexanol. The application of these surface-confined DNA oligomers as heterogeneous probes for the detection of polynucleotides (e.g., M13 phage DNA) is considered, with an emphasis on the elucidation of the relationship between the hybridization efficiency and the surface coverage and orientation of the probe molecules. Atomic force microscopy (AFM) and flow-injection quartz crystal microbalance (FI-QCM) were used in tandem to study the immobilization of the probe, to estimate the extent and efficiency of the hybridization of M13 phage DNA (7249 bases), and to examine the effect of using a different alkanethiol to reorient the preformed film for a higher hybridization efficiency. The surface density and the resultant hybridization efficiency were found to be highly dependent on the morphology and surface structure of the gold substrate as well as on the concentration of the solution used for the probe fabrication but much less dependent on the probe immobilization time. The lower limit of the hybridization efficiency was estimated to be about 1.1% which is an underestimate because only the resolvable circular features were included in the estimation. Although the duplex formed at the gold surface covered with only the thiolated DNA probe adopts exclusively the orientation in which the target loop is parallel with respect to the substrate surface, the predominant duplex orientation at the gold substrate modified with mixed self-assembled monolayers is tethered to the surface with a small tilt angle versus the surface normal. Visualization of the duplex orientation allows one to understand whether the Sauerbrey equation is valid for the interpretation of certain FI-QCM results. Although it is probably valid to use the Sauerbrey equation to calculate the amount of a polynucleotide at a surface covered only by the thiolated DNA probe, the practice might be questionable for that at the surface with the DNA/alkanethiol mixed SAM on the basis of our AFM images of the target orientations.

1. Introduction

Heterogeneous hybridization of DNA from free solution at oligonucleotide microarrays (DNA chips) could potentially become one of the most promising analytical techniques in molecular biology, because of the high specificity inherent in DNA base pairing, the sensitivity associated with various analytical detection schemes, and the declining cost for sensor fabrication.[1−5] Because conventional solid-phase hybridization performed on nitrocellulose or nylon membranes is time-consuming, many novel heterogeneous probes have been developed for faster and more sensitive detection. A great number of schemes for immobilizing single- and double-stranded DNA (ss- and ds-DNA) onto various substrate surfaces with different detection techniques (e.g., electrochemical, spectroscopic, quartz crystal microbalance, and atomic force microscopy) have been devised.[6−23] Among the various immobilization schemes, anchoring oligonucleotides onto the gold surface via an alkanethiol spacer or tether attached to either the 3′- or the 5′-end of the oligomer has received a considerable amount of attention. Part of the attention stems from the consideration of control and flexibility in forming self-assembled monolayers (SAMs) and from the possibility of producing a dense and compact surface coverage by the thiolated oligonucleotides. Thio-

(1) Lerman, L. *DNA Probes*: *Applications in Genetic and Infectious Disease and Cancer*; UMI: Ann Arbor, MI, 1986.
(2) Watson, J.; Gilman, M.; Witkowski, J.; Zoller, M. *Recombinant DNA*; 2nd ed.; W. H. Freeman and Company: New York, 1992.
(3) Chan, V.; Graves, D. J.; McKenzie, S. E. *Biophys. J.* **1995**, *69*, 2243−2255.
(4) Wetmur, J. G. *Crit. Rev. Biochem. Mol. Biol.* **1991**, *26*, 227−259.
(5) Henry, C. *Chem. Eng. News* **1999**, *10*, 7.
(6) Hegner, M.; Dreier, M.; Wagner, P.; Semenza, G.; Guntherodt, J. J. *Microelectron. Nanometer Struct.* **1996**, 1419−1421.
(7) Bard, A. J.; Xu, X.-H. *J. Am. Chem. Soc.* **1995**, *117*, 2627−2631.
(8) Wang, J.; Jiang, M. *Langmuir* **2000**, *16*, 2269−2274.
(9) Wang, J.; Cai, X.; Rivas, G.; Farias, P. *Anal. Chem.* **1996**, *68*, 2629−2633.
(10) Wang, J.; Palecek, E.; Nielsen, P.; Rivas, G.; Cai, X.; Shiraishi, H.; Dontha, N.; Luo, D.; Farias, P. *J. Am. Chem. Soc.* **1996**, *118*, 7667−7670.
(11) Mikkelsen, S. R.; Millan, K. M.; Saraullo, A. *Anal. Chem.* **1994**, *66*, 2943−2948.
(12) Thiel, A. J.; Frutos, A. G.; Jordan, C. E.; Corn, R. M.; Smith, L. M. *Anal. Chem.* **1997**, *69*, 4948−4956.
(13) Steel, A. B.; Herne, T. M.; Tarlov, M. J. *Anal. Chem.* **1998**, *70*, 4670−4677.
(14) Levicky, R.; Herne, T. M.; Tarlov, M. J.; Satija, S. K. *J. Am. Chem. Soc.* **1998**, *120*, 9787−9792.
(15) Herne, T. M.; Tarlov, M. J. *J. Am. Chem. Soc.* **1997**, *119*, 8916−8920.
(16) Huang, E.; Zhou, F.; Deng, L. *Langmuir* **2000**, *16*, 3272−3280.
(17) Kelley, S. O.; Barton, J. K.; Jackson, N. M.; Hill, M. G. *Bioconjugate Chem.* **1997**, *8*, 31−37.
(18) Kelley, S. O.; Barton, J. K.; Jackson, N. M.; McPherson, L. D.; Porter, A. B.; Spain, E. M.; Allen, M. J.; Hill, M. G. *Langmuir* **1998**, *14*, 6781−6784.
(19) Korri-Youssoufi, H.; Garnier, F.; Srivastava, P.; Godillot, P.; Yassar, A. *J. Am. Chem. Soc.* **1997**, *119*, 7388−7389.
(20) Peterlinz, K. A.; Georgiadis, R. M.; Herne, T. M.; Tarlov, M. J. *J. Am. Chem. Soc.* **1997**, *119*, 3401−3402.
(21) Hashimoto, K.; Ito, K.; Ishimori, Y. *Anal. Chem.* **1994**, *66*, 3830−3833.
(22) Patolsky, F.; Lichtenstein, A.; Willner, I. *J. Am. Chem. Soc.* **2000**, *122*, 418−419.
(23) Ihara, T.; Nakayama, M.; Murata, M.; Nakano, K.; Maeda, M. *Chem. Commun.* **1997**, 1609−1610.

10.1021/la001019i CCC: $20.00
Published on Web 01/18/2001

lated oligonucleotides of different base sequences have been used as a model system for studies of electron-transfer reactions through the DNA helices,[17] as linkers for synthesizing nanometer-sized systems,[24] as DNA sensors,[13,14,20,22,25−27] and recently as a means for screening protein/DNA interactions.[25] Tarlov and co-workers also conducted a systematic study, using a number of surface and analytical techniques, to address the distribution and orientation of the immobilized probe molecules and their hybridization with oligonucleotide targets.[13−15,20] Hegner et al. used atomic force microscopy (AFM) to measure the widths and lengths of relatively large thiolated oligonucleotides attached onto gold substrates.[28] It is now well established, from the results published by these researchers, that compact SAMs of DNA cannot be formed via simple chemisorption.[13−15,20] In addition, the electrostatic repulsion between the phosphate groups on adjacent oligonucleotides, instead of the van der Waals interactions existing among the alkyl chains of typical alkanethiol SAMs,[29] may partially be responsible for the relatively scarce distribution of the probe molecules. The surface density of thiolated double-stranded DNA varies with immobilization procedures and is highly dependent on the length of the DNA strand. For example, Hegner reported about 10% coverage by a thiolated DNA of 100 base pairs,[28] whereas Kelley et al. measured the surface coverage of a thiolated 15mer to be about 75% (with a density of 4.1×10^{-11} mol/cm^2).[17,18]

Owing to the above features that are unique to the immobilized thiolated DNA molecules, many DNA sensor developers have noticed that the formation of well-ordered DNA SAMs is not trivial,[17,28,30] and the immobilization procedures adopted depend on factors such as the number of bases on the probe and the type of the DNA targets to be detected.[13,14,20,22,25−27] In addition, there are quite a few ambiguities or controversies that are apparent among the papers published from different groups. For example, a 1992 paper by Okahata et al. showed that M13 phage DNA targets were hybridized at 100% efficiency, resulting in a large frequency decrease (ca. 500 Hz) monitored by a quartz crystal microbalance (QCM).[26] However, recent reports from several different groups show that smaller mass changes are generally observed in similar QCM experiments. For example, Uttenthaler and co-workers[31] had to use QCM crystals of very high fundamental frequencies to detect the frequency change caused by the same phage DNA target as in the work by Okahata and co-workers.[32] The crystal used in the work by Uttenthaler and co-workers (70 MHz)[33] was at least 60 times more sensitive than the 9 MHz crystal employed by Okahata and co-workers,[32] but the mass changes monitored in both studies were comparable. For the detection of oligonucleotide targets which have much smaller masses than the phage DNA, derivatization of the targets with liposomes by Willner and co-workers[22] or with gold nanoparticles by Zhou et al.[34] was carried out in order to increase the total mass of the target being detected. On the basis of the higher steric hindrance and stronger electrostatic repulsion arising from larger target molecules, one would expect that the hybridization efficiency should be lower for polynucleotides than for oligonucleotides. Another ambiguity in this field is concerned with the interpretation of the QCM experimental results. In a report by Fawcett et al.,[35] the validity of using the Sauerbrey equation to calculate the amount of hybridized target was questioned, because the targets, typically shown as macromolecules tethered with respect to the QCM crystal, may have extended beyond the acoustic wave envelope. The paper by Fawcett et al.[35] demonstrated experimentally that solvation and viscoelastic decoupling could concertedly affect the quantitative aspect of the QCM measurements of the hybridization of tethered DNA molecules. However, if the hybridized DNA duplex adopts an orientation that does not extend the DNA strand out of the acoustic wave envelope, the Sauerbrey equation is probably applicable in the semiquantitative estimate of the DNA hybridization.

Thus far, the relationship between the surface structure of the DNA probe (e.g., surface coverage and orientation) and the resultant hybridization for polynucleotides has not been fully elucidated. It is important to carry out such a study because this is related to the design of sequence-specific detection methods for analyzing large DNA/RNA molecules of bacterial and viral origins. Some of the aforementioned ambiguities may be resolvable if the orientation of the duplex DNA targets can be gauged and the quantities of the immobilized probe and hybridized target can be estimated. In this work, we used magnetic alternating current AFM (MAC-AFM) to examine the surface coverage and orientation of the probe as well as that of the target in an attempt to relate the surface structure of these molecules to the ultimate hybridization efficiency. AFM is known to be an indispensable tool in the study of immobilized DNA molecules.[36−39] The amount of probe immobilization and the extent of hybridization were also compared to that deduced by flow injection QCM (FI-QCM) experiments. Our work showed the direct visualization of the target orientation and determined several parameters affecting the hybridization efficiency (substrate morphology, probe concentration, probe immobilization time, and the use of "replacing alkanethiols"[14,15] for organizing the disordered probe molecules). The possibility of nonspecific adsorption of polynucleotides onto various surfaces was also studied and excluded by carrying out an experiment involving a mismatched DNA probe and target. The fundamental understanding from these studies should be helpful in the use of thiolated oligonucleotides for heterogeneous DNA sensor development and as building blocks for constructing interesting and important materials.

(24) Mitchell, G. P.; Mirkin, C. A.; Letsinger, R. L. *J. Am. Chem. Soc.* **1999**, *121*, 8122−8123.
(25) O'Brien, J. C.; Stickney, J. T.; Porter, M. D. *J. Am. Chem. Soc.* **2000**, *122*, 5004−5005.
(26) Okahata, Y.; Matsunobu, Y.; Ijiro, K.; Mukae, M.; Murakami, A.; Makino, K. *J. Am. Chem. Soc.* **1992**, *114*, 8299−8300.
(27) Whittemore, N. A.; Mullenix, A. N.; Inamati, G. B.; Manoharan, M.; Cook, P. D.; Tuinman, A. A.; Baker, D. C.; Chambers, J. Q. *Bioconjugate Chem.* **1999**, *10*, 261−270.
(28) Hegner, M.; Wagner, P.; Semenza, G. *FEBS Lett.* **1993**, *336*, 452−456.
(29) Ulman, A. *An Introduction to Ultrathin Organic Films*: *From Langmuir−Blodgett to Self-Assembly*; Academic Press: San Diego, 1991.
(30) Takenaka, S.; Yamashita, K.; Takagi, M.; Uto, Y.; Kondo, H. *Anal. Chem.* **2000**, *72*, 1334−1341.
(31) Uttenthaler, E. S. M.; Drost, S. *Ultrasensitive 39 to 70 MHz Quartz Crystal Microbalance Sensors for Detection of M13-Phages in Liquids*; Elsevier Science: San Diego, CA, 2000; p 147.
(32) Okahata, Y. M. Y.; Ijiro, K.; Mukae, M.; Murakami, A.; Makino, K. *J. Am. Chem. Soc.* **1992**, *114*, 8299−8300.
(33) Uttenthaler, E. S. M.; Mandel, J.; Drost, S. *Biosens. Bioelectron.* **2001**, in press.
(34) Zhou, X.-C.; O'Shea, S. J.; Li, S. F. Y. *Chem. Commun.* **2000**, 953−954.
(35) Fawcett, N. C.; Craven, R. D.; Zhang, P.; Evans, J. A. *Anal. Chem.* **1998**, *70*, 2876−2880.
(36) Lillehei, P. T.; Bottomley, L. A. *Anal. Chem.* **2000**, *72*, 189−196.
(37) Hansma, H. G.; Hoh, J. H. *Annu. Rev. Biomol. Struct.* **1994**, *23*, 115−139.
(38) Takano, H.; Kenseth, J. R.; Wong, S.-S.; O'Brien, J. C.; Porter, M. D. *Chem. Rev.* **1999**, *99*, 2845−2890.
(39) Bustamante, C.; Keller, D.; Yang, G. *Curr. Biol.* **1993**, *3*, 363−372.

2. Experimental Section

2.1. Materials. Ethylenediaminetetraacetic acid (EDTA) and tris(hydroxymethyl)aminomethane hydrochloride (Tris·HCl) were both from Sigma (St. Louis, MO), and NaOH and NaCl were obtained from Fisher Scientific (Tustin, CA). (3-Aminopropyl)-triethoxysilane (APTES) and mercaptohexanol (MCH) were purchased from Aldrich Chemicals (Milwaukee, WI). All solutions were prepared with water treated with a Millipore water purification system. M13mp18(+) and M13mp19(+) ss-phage DNA (abbreviated as M13 phage DNA or target DNA for the rest of the text) were purchased from Amersham Pharmacia Biotech (Piscataway, NJ) and Life Technologies (Rockville, MD), respectively. M13 phage DNA has 7249 bases, and the strand length should be around 2.46 μm if 0.34 nm is used as the base-pair spacing. A thiolated 17mer probe, SH-$(CH_2)_6$-5′-GTAAAACGACGGCCAGT-3′, and a thiolated 15mer probe, SH-$(CH_2)_6$-5′-GCGCGCGCGCGCGCG-3′, were acquired from Integrated DNA Technologies, Inc. (Coralville, IA). The first sequence is selective to both M13mp18(+) and M13mp19(+) phage DNA because the hybridization occurs outside of the multiple-cloning site, but the second sequence is not. Therefore, for this work both M13mp18-(+) and M13mp19(+) phage DNA samples are identical targets to the 17mer probe for the hybridization reaction. Cleland's Reductacryl reagent was acquired from Calbiochem-Novabiochem Co. (La Jolla, CA).

2.2. Solution Preparation. The Tris·HCl/EDTA (TE) buffer solution (10 mM Tris·HCl and 1 mM EDTA) has a pH of 7.0. TE/NaCl solutions were made by dissolving NaCl to a concentration of 0.1 M with the TE stock. The thiolated DNA probe stock in TE/NaCl solution was prepared inside a glovebox (Plas Labs, Lansing, MI). Dilute probe solutions were prepared daily using aliquots pipetted from the stock solution inside the drybox. M13 phage DNA solutions were prepared with TE/NaCl buffer outside of the glovebox.

2.3. QCM Crystals and AFM Gold Substrates. The QCM crystals used were AT-cut 7.995 MHz crystals that were coated with polished gold films (ICM Technologies, Oklahoma City, OK). Gold (111) substrates evaporated on mica were either purchased from Molecular Imaging (Phoenix, AZ) or generously provided by Dr. N. Tao (Florida International University).

2.4. Instrumentation. The AFM instrument and experimental conditions are the same as what we used previously.[16] QCM measurements were made using a CHI440 potentiostat/galvanostat (CH Instruments, Austin, TX). An acrylic QCM flow cell (ICM Technologies) with an internal volume of ca. 70 μL was used in conjunction with a six-port rotary valve (Valco Instruments Co., Houston, TX). The QCM cell and the oscillator circuit box were housed in a Faraday cage (Elchema Inc., Potsdam, NY). The TE/NaCl carrier solution loaded in a 10-mL plastic syringe was delivered with a Harvard Apparatus Pump11 syringe pump (Holliston, MA).

2.5. Procedures. 2.5.1. AFM. Vacuum-deposited gold (111) substrates were cleaned in the same fashion as we reported earlier.[16] The APTES-derivatized mica[37] was exposed to 15 μL of M13 phage DNA (2 μg/mL) for 5 min. The surface covered with the M13 phage DNA was then rinsed with water and imaged in a water solution.

To image ds-DNA formed from homogeneous hybridization of the M13 phage DNA with the probe, the duplex was first formed in a TE/NaCl solution containing 0.14 nM probe and 0.10 nM target at 55−75 °C for 30 min. Such a probe/target concentration ratio ensures that most, if not all, of the M13 phage DNA is hybridized. Gold substrates were then soaked in this solution for 4 h at room temperature. Prior to AFM imaging, the DNA-covered gold substrate was rinsed and dried in the same manner described above. For simplicity, this procedure is referred to as the immobilization of homogeneously formed DNA duplex.

To image the immobilized probe and the subsequently hybridized duplex (i.e., heterogeneously formed DNA duplex), a general scheme involves soaking a gold substrate into a probe solution for 4 h inside the drybox. We found that a more reproducible probe surface density could be obtained when the immobilization was carried out with the suspension of the Cleland's Reductacryl resin particles in the solution immersing the gold substrate. These resin particles contained immobilized dithiothreitol which can cleave the disulfide bond formed from the oxidation of the thiol groups by the residual oxygen in the solution. The surface was then subject to hybridization with the target of a specific concentration in a TE/NaCl solution. Probe concentrations of 0.005, 0.5, and 5 μM were employed to determine the optimal concentration that yielded the best probe coverage and the highest hybridization efficiency. We chose 0.5 μM as the concentration for comparative studies between AFM and FI-QCM.

In separate experiments addressing nonspecific adsorption of target DNA onto various surfaces, bare gold films, gold films covered with mixed MCH/thiolated 17mer SAMs, and gold films modified with MCH/thiolated 15mer SAMs were exposed to M13 phage DNA for 4 h. For preparation of mixed DNA/MCH SAMs, the procedure for probe immobilization was followed, with the modification of soaking the probe-covered gold films in 1 mM MCH for 1 h prior to the hybridization step.

2.5.2. QCM. The QCM crystal pretreatment follows our published procedure.[16] When the crystal was mounted onto the QCM flow cell, TE/NaCl carrier solution was introduced through the injection valve at a flow rate of 25 μL/min. Once a stable frequency baseline was established, the valve position was switched to the inject position to divert the analyte solution loaded into the 100 μL loop to the QCM cell. At this flow rate, it takes about 100 s for the injected sample to reach the QCM crystal and another 4 min for the carrier solution to completely replace the QCM cell content.

As for the use of QCM to monitor mass changes either at crystals covered with the probes or at crystals covered with a mixed SAM of the HS-ss-DNA probes and MCH, the QCM crystal surface was first modified with the respective species. For consistency, procedures for attaching the probe molecules to the QCM crystal or for the formation of the mixed SAM at the QCM crystal followed those used in the AFM studies.

The information obtained from QCM is more reflective of a process across the entire heterogeneous probe surface than that from AFM. Therefore, we relied more extensively on QCM in the investigation of the dependence of hybridization efficiency on the probe concentration and on the probe immobilization time. Because AFM studies indicated that immobilization of the probe in a 0.5 μM HS-ss-DNA solution yielded satisfactory hybridization, we first fixed the probe concentration and studied the effect of varying immobilization time. Four different immobilization times, 20 min, 2 h, 4 h, and overnight were examined. We then fixed the immobilization time at 4 h and explored the effect of probe concentration on the improvement of hybridization. Four different concentrations, 5 nM, 0.05 μM, 0.5 μM, and 5 μM were used, and the resulting hybridization efficiencies were compared.

3. Results and Discussion

3.1. Immobilization of Oligonucleotide Probe and Oligonucleotide−Polynucleotide Duplex. To understand the relationship between the surface coverage and orientation of the probe DNA molecules and the resulting hybridization efficiency, we used AFM to examine the surface coverage and molecular distribution of the immobilized probe molecules and employed FI-QCM to gauge the amount of immobilization. Figure 1a shows a representative AFM image of a gold surface that had been soaked in a 0.5 μM probe solution, whereas Figure 1b depicts a surface that had been treated with a 0.005 μM probe solution. Both images display relatively uniform distribution of the thiolated DNA probes (appearing as dots with sizes ranging from 26 to 40 nm). Although the size range is definitely greater than that of the strand width of ss-DNA,[40] it is not unusual because these images compare well with that of DNA attached to Au surfaces.[6,16,37,41−46] In fact, these values are in good agreement

(40) Lehninger, A. L.; Nelson, D. L.; Cox, M. M. *Principles of Biochemistry*; Worth Publishers: New York, 1993.
(41) Thundat, T.; Warmack, R. J.; Allison, D. P.; Ferrell, T. L.; Bottomley, L. A. *J. Vac. Sci. Technol., A* **1992**, *10*, 630−635.
(42) Yang, X.; Wenzler, L. A.; Qi, J.; Li, X.; Seeman, N. C. *J. Am. Chem. Soc.* **1998**, *120*, 9779−9786.
(43) Thundat, T.; Allison, D. P.; Warmack, R. J.; Doktycz, M. J.; Jacobson, B. K.; Brown, G. M. *J. Vac. Sci. Technol.* **1993**, *11*, 824−828.

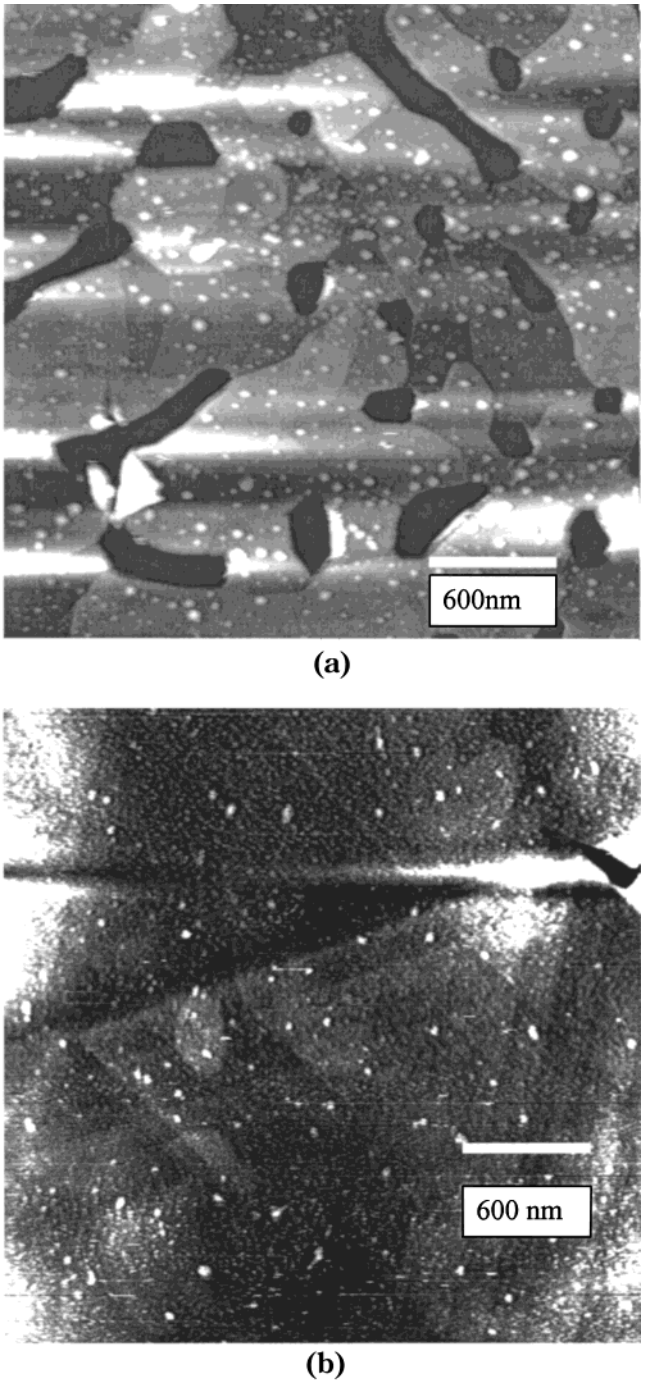

Figure 1. Topographical MAC-AFM images of (a) a Au(111) substrate covered with thiolated DNA probes produced by immersing the substrate in TE solution containing 0.5 μM probe and (b) a Au(111) substrate treated with TE solution containing 0.005 μM probe. Both images were obtained in DNA-free TE/NaCl buffer solutions.

with that of self-assembled thiolated ds-DNA on gold reported by Hegner et al.[28] The anomalously large dimensions of these thiolated DNA molecules can be attributed to the image broadening effect caused by the tip interaction with the wiggling DNA strands.[18,28] Another possibility is that the DNA probe molecules are actually lying flat onto or adopting different tilt angles with respect to the surface, because of the nonspecific interaction between the bases of the HS-ss-DNA and the gold surface, as suggested by Tarlov and co-workers.[13−15,20] The varying orientation might therefore be the origin of the size distribution. Nevertheless, our AFM images demonstrated that the procedure used for the HS-ss-DNA probe immobilization is successful. The relative standard deviation of the surface density, deduced from counting the dots across unit areas in seven different immobilization experiments, is 12.4%. This reproducibility could be attributable to the solution preparation and immobilization under anaerobic environment and the use of reductacryl for cleaving disulfide bonds between two thiolated DNA molecules. A comparison between images a and b of Figure 1 indicates that the use of a more concentrated HS-ss-DNA was more favorable to denser probe coverage. The average surface density of the probe molecules was estimated to be 1.1×10^{10} molecules/cm^2 in Figure 1a, whereas that measured from Figure 1b was 3.0×10^9 molecules/cm^2. The trend is also consistent with that observed in separate FI-QCM experiments described below. The HS-ss-DNA film is not compact because there are still many uncovered gold regions. This is not surprising because many researchers have observed similar phenomena.[13,14,20,22,25−27]

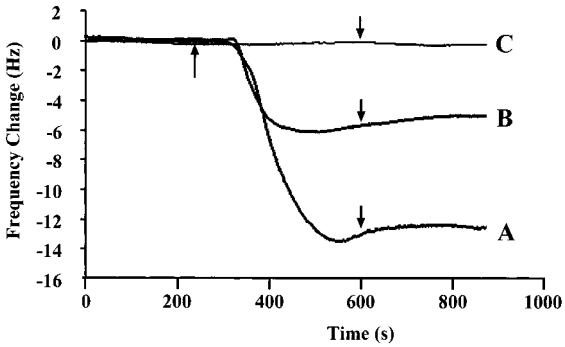

Figure 2. Time-resolved QCM responses to the injections of 100 μL of a TE solution containing 0.5 μM (A) and 0.005 μM (B) of thiolated DNA probe solutions are shown. Injection of 100 μL of a TE solution into the QCM cell is also shown (C). Arrows indicate the times when injections were made and when the injected samples were completely replaced by the carrier solution.

The final surface coverage was also found to be dependent on the topography and surface structure of the gold surface. For example, the surface coverage at polycrystalline gold surfaces such as that on the QCM crystals is greater. Figure 2 shows time-resolved QCM responses corresponding to the injections of 100 μL of 0.5 and 0.005 μM thiolated probes into a TE carrier solution. Again, the higher HS-ss-DNA concentration resulted in a greater amount of molecules to attach to the gold surface. In Figure 2, the time lapse between the injection and the onset of the frequency decrease correlates well with the time needed for the injected sample to reach the crystal. This suggests that the adsorption of the thiolated DNA is essentially instantaneous. Interestingly, when the injected sample has been completely replaced by the carrier solution (shown by the arrows in Figure 2) there appears to be a small frequency increase (mass loss). We believe that the small frequency increase is due to the detachment of the nonspecifically or loosely bound thiolated DNA molecules that were washed off by the carrier solution. However, the mass remains constant for at least 7 h in

(44) Hansma, H. G.; Sinsheimer, R. L.; Groppe, J.; Bruice, T. C.; Elings, V.; Curley, G.; Beznilla, M.; Mastrangelo, I. A.; Hough, P. V. C.; Hansma, P. K. *Scanning* **1993**, *15*, 296−299.
(45) Hansma, H. G.; Revenko, I.; Kim, K.; Laney, D. E. *Nucleic Acids Res.* **1996**, *24*, 713−720.
(46) Hansma, H. G.; Golan, R.; Hsieh, W.; Lollo, C. P.; Mullen-Ley, P.; Kwoh, D. *Nucleic Acids Res.* **1998**, *26*, 2481−2487.

a quiet probe solution, suggesting that the attachment of DNA film to the crystal is robust.

From the time-resolved QCM response, the surface coverage by the immobilized probes can also be estimated. In Figure 2, a 12.4 Hz decrease (or a mass increase of 16.8 ng) corresponds to a surface density of 1.58×10^{12} molecules/cm^2. This corresponds to a surface coverage of about 23%. This value also shows that the probe density at the QCM crystal is much greater than that at the AFM gold substrate (1.1×10^{10} molecules/cm^2). A possible explanation can be made using the drastic difference in the Au grain sizes between the QCM crystal (about 55−75 nm wide, measured by AFM) and the Au film on mica (typically 300−500 nm wide). The significantly smaller Au grains on the QCM crystals mean that there are more grain boundaries and/or dislocations. These surface structures or features are known to be more active than those on the terrace.[47] Conceivably, a less smooth surface can minimize the steric and electrostatic interactions between neighboring probe molecules. Consequently, the number of thiolated DNA molecules immobilized onto the small gold terraces on the QCM crystal will be greater than that on the much smoother and larger Au(111) islands.

One of the objectives of this work is to directly visualize the orientation of the DNA duplex produced from the hybridization of the target with the immobilized probe molecules. This objective prompted us to choose vector DNA as the target because the circular shape of vector DNA enables one to resolve the attached target clearly. However, differentiation of the circular feature from the topographical background of the substrate is largely dependent on the orientation of the DNA duplexes, which in turn is governed by the orientation adopted by the probe. For example, plasmid or other linear DNA molecules electrostatically attached to the substrate surface generally orient themselves parallel to the underlying surface. Figure 3a is an AFM image of M13 phage DNA immobilized onto an APTES-derivatized mica. The intertwining of DNA strands is due to the electrostatic attraction of the negative charges on the DNA backbone by the randomly distributed positive charges on the APTES-derivatized mica. The disordered DNA structures are common because electrostatic interaction does not render control to the immobilization process.[37,41−43,45,46,48] However, the relatively high density of the positively charged sites on the derivatized mica resulted in attachment of the DNA molecules with their strands lying parallel to the surface. Nevertheless, the fixation and confinement of a major portion of a DNA strand onto the surface allows one to clearly resolve the DNA molecules and to measure the strand width. In Figure 3a, the strand width was determined to be 13 ± 2 nm, which is in good agreement with values in other AFM studies of DNA.[6,16,37,41−46]

If a polynucleotide is affixed to the surface only at one end via a tether, its flexible portion in solution is significantly longer than that of a tethered oligonucleotide. Therefore, the image broadening effect might be even more pronounced than that encountered in imaging tethered oligonucleotides or alkanethiols. Moreover, if the loop of a vector DNA is perpendicular to the surface or tilted at an angle with respect to the surface normal (alkanethiols are tilted at about 27°)[29,49,50] it could blur the observed images as the tip would just raster over the topmost portion of a tilted DNA loop which is very flexible and compressible.

In an attempt to study the AFM tip interaction with the solution ends of the wavering polynucleotides, we first carried out an AFM experiment to image the immobilized duplexes that were formed through a homogeneous hybridization between the HS-ss-DNA and the polynucleotide target. The HS-ss-DNA was in excess to ensure a full conversion of all the polynucleotides to the corresponding duplexes. As a result, the final solution consisted of the oligomer−polynucleotide duplexes and unconsumed HS-ss-DNA probe. Figure 3b shows an AFM image, acquired in a DNA-free TE/NaCl solution, of a Au substrate that had been immersed in such a solution. Although a large portion of the surface was covered with the unconsumed HS-ss-DNA from the solution, certain regions of the surface showed the presence of the immobilized duplexes. As expected, the image broadening effect, arising from the longer strand of the polynucleotide, was more severe and resulted in a less clear image of the duplexes. The cross-sectional contour across a typical tethered loop is about 21 nm (Figure 3b) which is larger than both the height variation of the underlying Au surface and the depth of a flat-lying DNA strand (in Figure 3a and in Figure 4a described below, the height variation of a flat DNA strand is typically 2−3 nm). This value probably does not reflect accurately the height of the tilted loop because the tip might have compressed the DNA loop during imaging. Interestingly, the enlarged image of a given duplex (Figure 3c) revealed that the circular feature of some duplexes could be vaguely resolved as a loop tethered to the substrate surface. Because of the image-broadening effect associated with the tip/sample interaction, the strand width can only be estimated to be ca. 160−200 nm in Figure 3c. The perimeter of the circle seems to resemble the configuration in which two parallel strands of a loop extend into the solution.

In a separate FI-QCM experiment, 100 μL of the mixture was injected into the QCM cell and the mass change was recorded. The total mass increase was found to be 40.5 ng (ca. 30 Hz), which is much more pronounced than that shown in Figure 2. It is clear that coadsorption of the thiolated hybrids and the unconsumed probes resulted in a higher frequency change. The uncertainties of using the Sauerbrey equation for quantification because of different DNA orientations will be elaborated below in connection with the discussion of the quantification of the target molecule hybridized heterogeneously. Despite the inapplicability of the Sauerbrey equation for quantifying tethered and solvated biomolecules, the different frequency changes from the QCM measurements support our AFM findings.

3.2. Hybridization of Polynucleotide at Gold Surfaces Covered with Self-Assembled Oligonucleotide Probe. We performed AFM and QCM studies to assess the hybridization efficiency of the immobilized thiolated probe for polynucleotide. Figure 4a is a representative AFM image showing the result of exposing a HS-ss-DNA-modified gold substrate to a 0.15 nM solution of M13 phage DNA. As can be seen, several circular M13 phage DNA molecules are clearly resolvable. The strand width in Figure 4a is 25−35 nm. Such a range is in close agreement with that in Figure 3a, suggesting that most of the vector DNA was anchored to the gold surface laterally and tightly.

(47) Somorjai, G. A. *Chemistry in Two Dimensions Surfaces*; Cornell University Press: Ithica, NY, 1981.
(48) Han, W.; Dlakic, M.; Zhu, J. Y.; Lindsay, S. M.; Harrington, R. E. *Proc. Natl. Acad. Sci. U.S.A.* **1997**, *94*.
(49) Porter, M. D.; Bright, T. B.; Allara, D. L.; Chidsey, C. E. D. *J. Am. Chem. Soc.* **1987**, *109*, 3559−3568.
(50) Dubois, L. H.; Nuzzo, R. G. *Annu. Rev. Phys. Chem.* **1992**, *43*, 437−463.

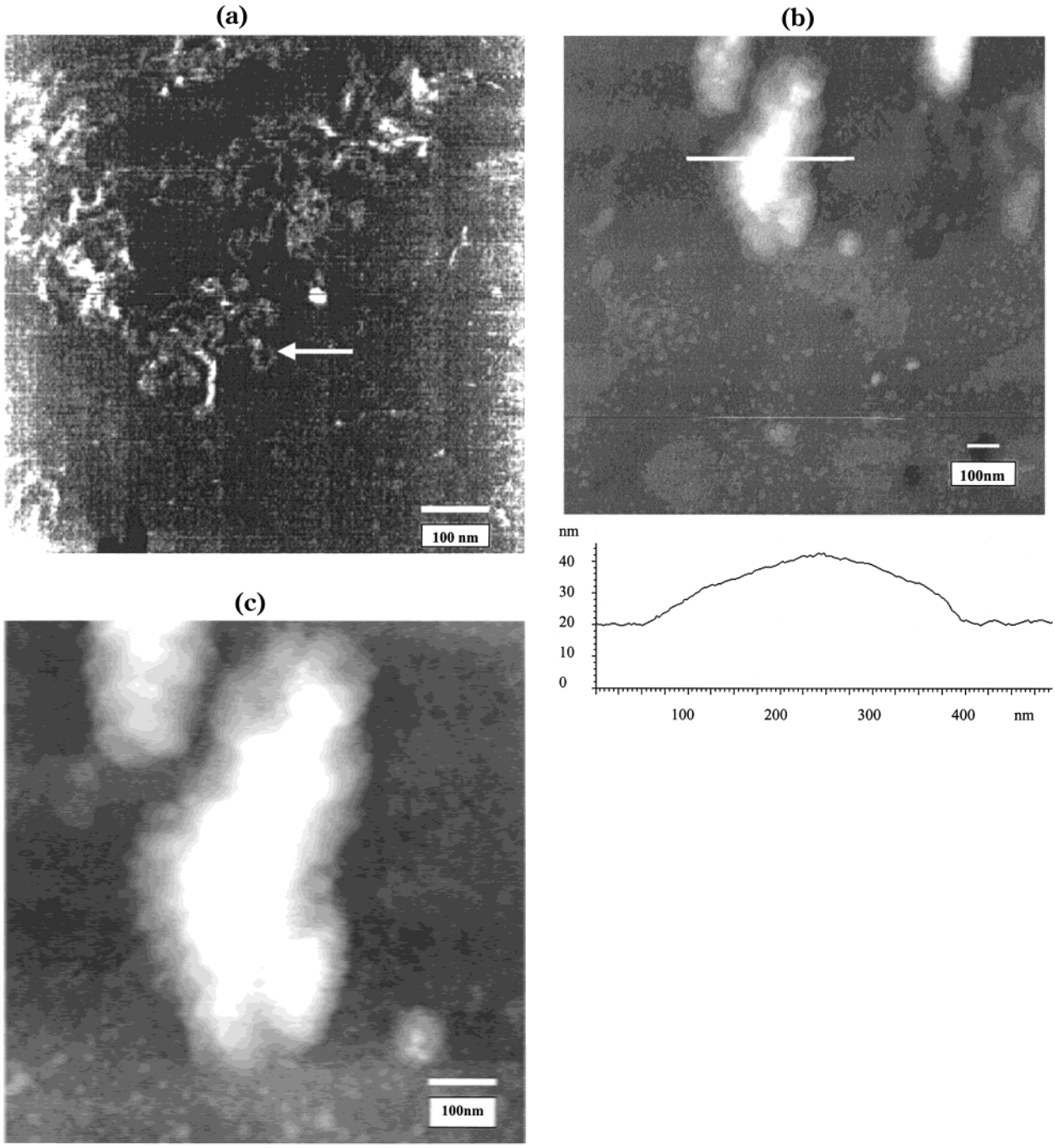

Figure 3. Topographical MAC-AFM images of (a) M13 phage DNA electrostatically adsorbed onto an APTES-treated mica substrate and (b) a Au(111) substrate that had been exposed to a mixture containing homogeneously formed duplexes between the probe and the M13 phage DNA as well as the unhybridized thiolated DNA probes. The cross-sectional contour shows the height variation across the tethered DNA loop indicated by the white bar. Image c is an enlarged depiction of one of the homogeneously formed duplexes tethered onto the Au(111) substrate.

The cross-sectional contour across the DNA loop identified by the thick arrow in Figure 4a has a height of about 3 nm. Therefore, the DNA loops appear to be almost perfectly aligned with the substrate surface. The comparison of this height difference to that in Figure 3b clearly indicates that the two images have different surface orientations. We also attempted to estimate the strand length of the hybridized DNA. Although there is a large uncertainty in deducing the length of a vector DNA in Figure 4a because the strand is not straight, we obtained a value of about 1.68 μm for the target molecule identified by the thick arrow in Figure 4a. Though shorter than the theoretical value (2.46 μm), the discrepancy is not significant considering that parts of the strand were hinged over the terrace(s) and could not be measured.

In a separate experiment, we replaced the above probe with a thiolated 15mer whose sequence (see Experimental Section) is not complementary to the target and carried out the same heterogeneous DNA sensing experiments. Shown in Figure 4b is an AFM image of a gold substrate covered with the 15mer probe that had also been soaked in the target solution for the same amount of time under identical experimental conditions. The absence of the circular structure indicates that the polynucleotides in Figure 4a are not due to nonspecific DNA adsorption. Therefore, based on the general agreement in terms of

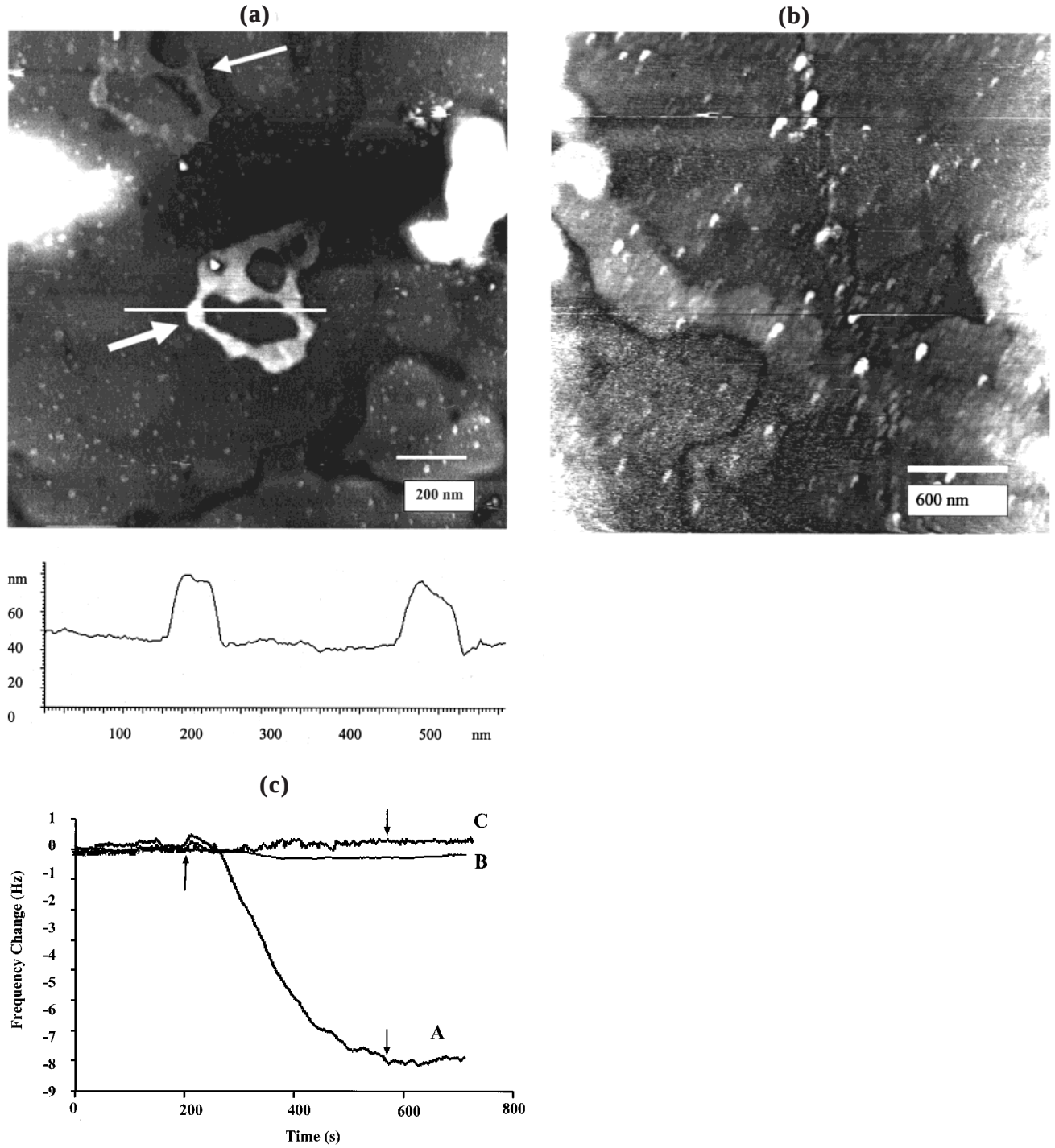

Figure 4. (a) Topographical MAC-AFM image of heterogeneously formed duplexes resulted from hybridization of probe molecules with M13 phage DNA in TE/NaCl solution. The AFM image was obtained in a DNA-free TE/NaCl solution. The cross-sectional contour shows the height variation across the flat-lying loop indicated by the white bar. (b) AFM image of a gold substrate covered with thiolated 15mer upon the same treatment as in (a). (c) Time-resolved QCM response to the injection of 100 μL of 0.15 nM M13 phage DNA into the QCM cell housing a QCM crystal covered with probe DNA (curve A) is shown. Curve B was the response when the same solution was injected into the QCM cell housing a bare QCM crystal, and curve C was obtained with a mismatched 15mer probe for the same target. Arrows indicate the times when injections were made and when injected samples were completely replaced by the carrier solution.

the length, width, and shape of the observed feature with the theoretical predictions as well as the experiment using the mismatched DNA probe and target, we are confident that hybridization does take place at the heterogeneous probe surface and AFM can be used as an effective detector.

Several additional points are noteworthy from analyzing Figure 4a: (1) the resolved duplex exclusively adopts the orientation in which the DNA loop is parallel to the gold substrate, (2) the duplexes were most likely to be found at the gold grain boundaries, and (3) the majority of the thiolated DNA probes have not been utilized (hybridized). The observation of such duplex orientation is actually not surprising considering the well-known interaction between the DNA bases and the gold surfaces.[6,13−15,20,25,27,30] Such interaction apparently operates in a similar fashion as the electrostatic attraction between a positively charged mica surface and a DNA molecule (Figure 3a). The difference here is that the effect of the more uniform

coverage of the unhybridized probe molecules and the relatively low hybridization efficiency (discussed below) spreads the target distribution. The explanation for the appearance of the hybrids at the grain boundaries is as follows. On a large and smooth terrace, the close spacing of probe molecules hampers the movement of target molecules toward probe molecules for hybridization. Even if there is enough space for the target molecules to approach the probe-covered surface, the flexibility of the DNA in the vicinity of the surface might not be as high as that of DNA in the bulk solution. Consequently, the short portion on the target that is complementary to the probe sequence might not be perfectly aligned with the probe molecule for hybridization. On the contrary, probes situated at the edges of the grain boundaries are more accessible. In fact, the hybridization efficiency can be estimated by comparing the sensing surface before and after the hybridization process. As mentioned above in section 3.1, the probe surface density is about 1.1×10^{10} molecules/cm^2. The hybridization efficiency can be estimated by dividing the duplex surface density by the probe surface density examined. The hybridization efficiency was found to be about 1.1%. Such a hybridization efficiency is lower than that for hybridization with oligonucleotide targets.[6,13−15,20,23,25,30] However, our recent improvement of these AFM images by using an additional hybridization involving DNA-capped gold nanoparticles[51] allowed a more accurate determination of the hybridization efficiency (about 16%) and indicated that the 1.1% deduced by including only the clearly resolvable circles is an underestimate. In any case, the hybridization efficiency is lower than that between oligonucleotide probes and oligonucleotide targets[13−15] and suggests that the weak interactions between DNA bases and the gold surface, together with the steric hindrance of the adjacent probe molecules, are not highly favorable for duplex formation.

We also used FI-QCM to estimate the amount of target molecules hybridized by the immobilized probe molecules and the extent of hybridization. Curve A in Figure 4c is a time-resolved QCM response obtained from injecting 100 μL of 0.15 nM M13 phage DNA into a QCM cell containing a QCM crystal covered with probe molecules. Compared to the two control experiments involving a bare gold-coated crystal (curve B) and a crystal covered with the sequence-mismatching 15mer (curve C), it is again clear that the possibility of nonspecific target adsorption can be excluded. Thus, the conclusion drawn from the QCM measurements is in line with that derived from the AFM imaging. The mass increase in Figure 4c corresponds to a target density of 1.9×10^{10} molecules/cm^2. Interestingly, the hybridization efficiency calculated by dividing the target density by the probe density (1.58×10^{12} molecules/cm^2 from Figure 2), 1.2%, is not higher than that estimated from the AFM experiments. This suggests that although the morphology of the gold film on the crystal favors the attachment of more abundant probes the ultimate hybridization at such a surface is not dramatically improved, possibly because of the steric hindrance and electrostatic repulsion to the polynucleotide targets by the densely packed unhybridized probe molecules.

One of the ambiguities regarding QCM detection at a crystal covered with thiolated DNA probes is that the Sauerbrey equation could be invalid. This argument is based on the premise that tethered probes could cause the solvated duplexes to extend into the solution beyond the acoustic wave envelope.[35] Interestingly, as evidenced by the AFM image in Figure 4a, when all the target molecules opt for an orientation in which the strands are parallel to the underlying substrate viscoelastic effects associated with the tethered macromolecules are probably negligible. Our estimate of the hybridization efficiency using the Sauerbrey equation should be meaningful in this particular case because estimates of the hybridization efficiency from both measurements do not differ significantly. However, as already discussed in the description of Figure 3b and will be described below regarding the reorientation of the probe and target molecules using mixed SAMs, when the tethered configuration is encountered, caution should be exercised. Therefore, although the use of the Sauerbrey equation in Okahata's work[26] for quantification is probably appropriate the general depiction of the probes as tethered molecules is incorrect. Furthermore, there is an obvious discrepancy between the magnitude of the frequency decrease in Figure 4c and that shown by Okahata et al.,[26] even though our experimental procedure and instrumental design are similar. Our frequency change is at least 2 orders of magnitude lower than that reported by Okahata and co-workers. Other groups[33,34,52] also observed low QCM signals from the hybridization of target DNAs with immobilized thiolated oligonucleotides. Because our experimental results are consistent with the observations of these groups, we suspect that there must be some artifacts associated with the measurements performed by Okahata and co-workers.[26] We noticed that deionized water rather than a buffer solution with high ionic strength was employed in ref 32. Because the phage DNA are polyanions and are typically made in a buffer solution and QCM response is known to be subject to solution conductivity change,[53] the anomalously large frequency change in ref 32 could be due to the change of solution conductivity brought by the addition of the DNA solution to the small volume of pure water immersing the QCM crystal. For example, when we injected 100 μL of 0.05 M NaCl dissolved in a TE buffer into a deionized water carrier solution we observed a frequency change of 52 Hz.

The last experiment in this section is concerned with the effect of probe concentration and immobilization time on the final hybridization efficiency. Figure 5a is a plot of the amount of hybridized targets measured by QCM versus the logarithm of the probe concentration. As expected, the probe density produced from a lower probe concentration caused the attachment of fewer target molecules. However, the amount of hybridization is below the QCM detection limit when the QCM crystal that had been immersed in a solution of a much higher probe concentration (5000 nM) was used. Taking into account the steric hindrance to the heterogeneous hybridization and the fact that targets exist at grain boundaries (see Figure 3a), it becomes clear that a surface densely covered with thiolated probes could actually be detrimental to the hybridization efficiency. From Figure 5a, it appears that the probe concentration of 500 nM yielded an optimal surface density for the highest hybridization efficiency.

Figure 5b is a plot of the amount of hybridization versus the time used for soaking the QCM crystal in a probe solution. Although longer soaking times yielded slightly higher hybridization, the improvement is not significant. It is obvious that a short soaking time (e.g., 20 min) allows a sufficient amount of probe molecules to be anchored. In other words, with the optimal probe concentration the

(51) Han, S.; Lin, J.; Zhou, F.; Vellanoweth, R. L. *Biochem. Biophys. Res. Commun.* **2000**, *279*, 265−269.

(52) Patolsky, F. L. A.; Willner, I. *J. Am. Chem. Soc.* **2000**, *122*, 418−419.

(53) Dunham, G.; Benson, N. H.; Danuta, P.; Jiri, J. *Anal. Chem.* **1995**, *57*, 267−272.

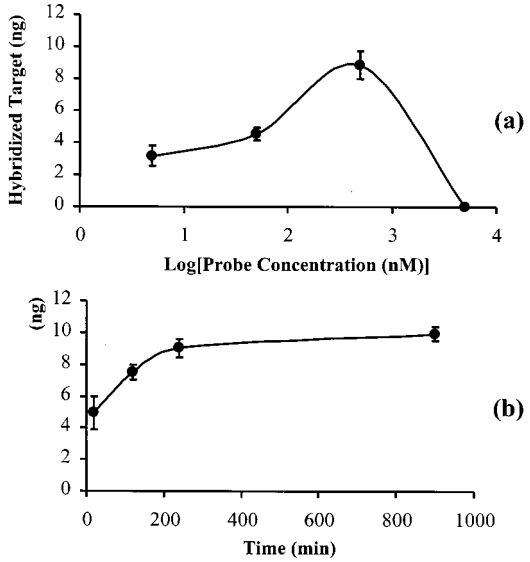

Figure 5. QCM mass changes plotted (a) as a function of the logarithm of the probe concentration used for the immobilization and (b) as a function of probe immobilization time. The standard deviations for each concentration or time were plotted as error bars. Three replicates were made for each measurement.

immobilization is effective and rapid. This point is in line with the steep frequency decrease shown in Figure 2. Therefore, throughout this work, for time effectiveness, 4 h (or 240 min) was chosen as the time for immobilizing the probe onto the QCM crystal or the AFM substrate.

The above study on the probe concentration and immobilization time is useful because the detection limit of QCM toward DNA hybridization is mainly limited by the hybridization efficiency. Without resorting to other alternative approaches,[22,31] it is imperative to operate the QCM under the most favorable hybridization conditions.

3.3. Hybridization of Polynucleotide at Gold Surfaces Modified with Mixed SAMs Containing Alkanethiols and Thiol-Tethered Oligonucleotide. As aforementioned, the hybridization efficiency of the surface-confined probes for polynucleotides is not high. For practical application, the immobilization efficiency must be improved in order to fabricate useful heterogeneous DNA sensors. We explored the strategy originally pioneered by Tarlov and co-workers[13−15] by replacing the disordered probes with alkanethiol molecules. As discovered by these researchers, the hybridization efficiency between an oligonucleotide probe and an oligonucleotide target was found to be enhanced by soaking the surface modified with the probe molecules in a mercaptohexanol (MCH) solution for various amounts of time.

Figure 6 is an AFM image showing the duplexes heterogeneously formed between M13 phage DNA targets in solution and the immobilized oligonucleotides that are mixed with MCH. The mixed SAMs were fabricated by immersing the probe-covered gold surface into a 1 mM MCH solution for 1 h. We found that a shorter time (e.g., 5 min) did not result in a complete coverage of the bare gold regions by the MCH. In Figure 6, because of the protrusion of the tethered duplexes it is more difficult to resolve the unhybridized probes or MCH molecules around the large polynucleotide strands. Also in Figure 6, we did not observe any circular features like that in Figure 4a, in which the surface-confined target DNA molecules were attached with their loops parallel to the substrate surface. Instead, the features in Figure 6 resemble the oblong-shaped duplexes in Figure 3b. This development is consistent with the model proposed by Tarlov and co-workers who suggested that the attachment of MCH to the unoccupied gold regions would competitively replace certain nonspecifically adsorbed probes.[15] Such a competitive displacement will also prop up some randomly oriented probe molecules. The net result is that the hybridization efficiency will be improved because of these surface processes. As can be seen in Figure 6, the duplex whose cross-sectional contour was shown by the white bar appeared to have its loop slightly tilted with respect to the surface normal. Because most of the duplex loops (which are larger and longer than the oligonucleotides used in the work by Tarlov and co-workers[13−15]) can be in the sway motion, the image-broadening effect is severe. The strand width can only be estimated to be 70−140 nm. Nevertheless, this range is in good agreement with that estimated from the immobilized homogeneously formed duplexes (about 160−200 nm in Figure 3b). In images such as that in Figure 6, it is difficult to estimate the number of duplexes within a unit area. Using the length of the topmost portion of a loop estimated from Figure 3c (about 0.33 μm), it appears that there are about 6 duplexes across the area shown in this image. However, such an approximation is crude because the length of the topmost portion of each molecule could vary. Another interesting comparison can be made between the height variation in Figure 6 and that in Figure 3b. In Figure 6, the height difference between the MCH solution termini and the topmost region of a strand ranges between 14 and 33 nm. Such a height difference compares well with that between the topmost portion of a tethered DNA loop and the

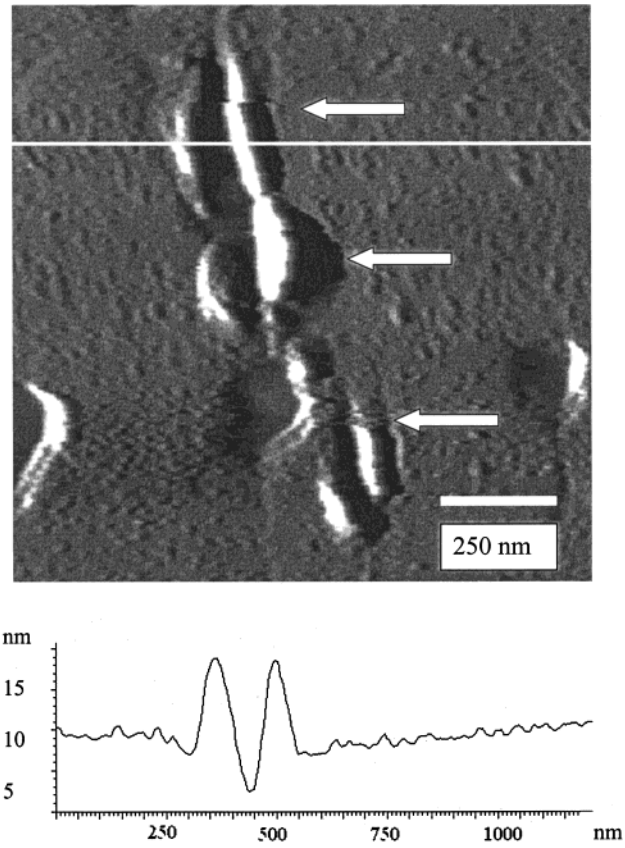

Figure 6. Topographical MAC-AFM image showing the heterogeneously formed duplexes between M13 phage target DNA in solution and the probe molecules that are mixed with self-assembled MCH molecules. The mixed SAMs were fabricated by immersing the substrate covered with DNA probes into a 1 mM MCH solution for 1 h. The cross-sectional contour shows the height difference between the tethered DNA and the MCH molecules.

underlying gold surface (Figure 3b). Therefore, we are convinced that the oblong features shown in Figure 6 most likely originated from DNA loops that possess a surface orientation similar to that in Figure 3b.

Because the area mapped in Figure 6 is about 54% of that examined in Figure 4a and it seems that an increase by 3-fold in the number of hybridized targets was observed in Figure 6, the hybridization efficiency is therefore improved to about 6.2%. However, considering that the competitive displacement of disordered probe molecules by an alkanethiol can reduce the total number of DNA molecules at the surface,[13−15,25,27,30] there might be fewer probe molecules in the mixed SAMs during the hybridization step. This means that the hybridization efficiency may have increased more significantly.

Finally, we carried out an experiment in which 100 μL of 0.15 nM M13 phage DNA was injected into a QCM cell that contained a QCM crystal covered with the MCH/thiolated probe mixed SAMs. We found that the mass change is actually smaller than that occurring in the hybridization at a QCM crystal covered with only thiolated probe molecules. However, it is important to reiterate that given the complication caused by the extension of the tethered macromolecules out of the acoustic wave envelope (as suggested by the above AFM results) it is difficult to know the exact hybridization efficiency. The QCM measurements are ambiguous in probing the important parameters affecting the hybridization efficiency at the thiolated DNA/alkanethiol mixed SAM films.

4. Conclusion

This study demonstrated that the use of AFM and flow-injection QCM in tandem can provide important information about the surface coverage and orientation of the thiolated oligonucleotide probe as well as factors affecting the hybridization efficiency. Whereas AFM allows direct visualization of orientations of both probe and target DNA molecules, QCM provides a means to semiquantitatively measure the amount of immobilized probe molecule and that of the hybridized duplexes. The AFM images clearly indicate that the DNA hybrid formation at the heterogeneous sensor preferentially occurred at the gold grain boundaries, suggesting that the steric hindrance by the adjacent DNA probe molecules plays an important role in governing the amount of hybridization. Visualization of the duplex orientation allows one to understand whether the Sauerbrey equation is valid for the interpretation of certain FI-QCM results. Although it is probably valid to use the Sauerbrey equation to calculate the amount of a polynucleotide at a surface covered only by the thiolated DNA probe, such a treatment might be questionable for that at the surface with the mixed DNA/alkanethiol SAM, based on the AFM images of the target orientations. Both AFM and QCM studies indicate that the hybridization efficiency is low. This is not unexpected when the disorganization of probe molecules and the steric hindrance at the heterogeneous probe surface toward hybridization of bulky polynucleotides are considered. Alteration of the probe surface density and orientation for a better hybridization efficiency is therefore desirable. We conducted a preliminary study to change the probe orientation by displacing the disordered DNA probes with MCH. The hybridization efficiency at mixed SAMs of MCH and HS-ss-DNA improved the overall hybridization by 5-fold to about 5−6%. However, the hybridization efficiency is not as high as that between oligonucleotide probe and oligonucleotide target. We are now in the process of designing surfaces by selectively attaching thiolated DNA probes with a controlled spatial distribution in an attempt to hybridize polynucleotides at higher hybridization efficiencies.

Acknowledgment. Partial support for this work by the NIH-SCORE subproject (Grant No. GM08101), from the donor of the Petroleum Research Funds, administered by the American Chemical Society, and the NSF-CRUI program (Grant No. DBI-9978806) is gratefully acknowledged. We also thank Dr. N. Tao (Florida International University) for providing some of the gold films used in this research and Dr. R. Vellanoweth for helpful discussions.

LA001019I